ICAS 2016
30th Congress of the International Council of the Aeronautical Sciences
DCC, Daejeon, Korea ; September 25-30, 2016

FLIGHT TESTS OF THE VISION-BASED TARGET SENSING AND APPROACHING

Sungwook Cho*, Yeundeuk Jung, David Hyunchul Shim***
***Korea Advanced Institute of Science and Technology,**
****Korea Aerospace Research Institute**
Swcho84@kaist.ac.kr; jyd@kari.re.kr; hcshim@kaist.ac.kr

Keywords: *Target sensing, Multi-feature detector, Time-to-go, Direct visual servoing, Flight test*

Abstract

In this paper, we propose the visual target sensing algorithm using the feature fusion and validate by flight tests. Sensing algorithm is divided by two parts: multi-feature detector and fusion. Multi-feature detector consists of the point-like feature, texture, and shape detector. The fusion part is implemented in the sequential update step of the Kalman filter-based tracking algorithm. This approach can detect the target robustly in the real outdoor environment that the scale of the target is changing. Furthermore, we designed the time-to-go-based longitudinal guidance controller with the direct visual servoing and performed the Open-loop and closed-loop flight tests by using the quadrotor and fixed-wing UAVs. The open-loop test is performed by using the quadrotor UAVs for validating the visual sensing algorithm; the closed-loop test is repeatedly performed by using the fixed-wing UAVs with the direct visual servoing-based guidance in the same environment. Finally, we analyze the results that approaching the target based on the circular error probability (CEP).

1 Introduction

Recently, the mission of the unmanned aerial vehicle (UAV) performed by using the vision sensor system has been increased dramatically. The vision sensor system including the onboard embedded computer or off-board transmitting-based processing can deal with the source image to the valuable information easily almost in real time. There are many requirements to perform the image processing to convert the pixel information into the interesting data such as the target`s Geo-location, the bearing and azimuth angle etc. These data are used to generate the environment information for the higher-level algorithm or converted to the reference fed into the visual guidance loop. To satisfy its performance requirements, the reliable target sensing algorithm is strongly needed. Many researches have been studied for the visual sensing algorithm, but most of them are used the single feature detector. Generally, the target in the real world, not artificially generated, has many features such as the point-like, the texture including the color and shape, the edges etc. When using the single feature, it may be failed or flickered in the uncertain dynamic environments. Especially, the single feature detector is vulnerable to changing the camera`s heading, the magnitude of the sun light or the amount of clouds

To overcome the problem more practically, the novel visual sensing algorithm by using multi-features is proposed in this paper. Furthermore, the time-to-go-based longitudinal guidance law with the direct visual servoing scheme is proposed. The proposed system is verified by performing the flight test repeatedly and analyzed statistically by using the circular error probability (CEP) scheme.

This paper is organized as follows. In section 2, the visual sensing algorithm is presented based on the multi-feature detector and the sequential measurement fusion scheme based on Kalman filter. In section 3, the time-to-go-based longitudinal guidance law with the direct visual servoing is described. Section 4 represents the flight test and the analysis results.

2 Multi-Feature-based Visual Sensing for the Designated Target

In this paper, we developed the target sensing algorithm by using three feature: points, texture and edges. The designated target information is assumed as the prior knowledge given from the single image before the flight test. Although it does not quite equal the real one, we can make good use of it. The target image and the developed one by using the inflatable material are shown in Fig. 1. As shown in this figure, it has complex features. First, it is quite dart overall. Furthermore, it has the similar color compared with the environment. However, it has a distinct texture and vertical edges. These prior information can be helpful when configuring the feature selection and developing the image processing algorithm.

(a)

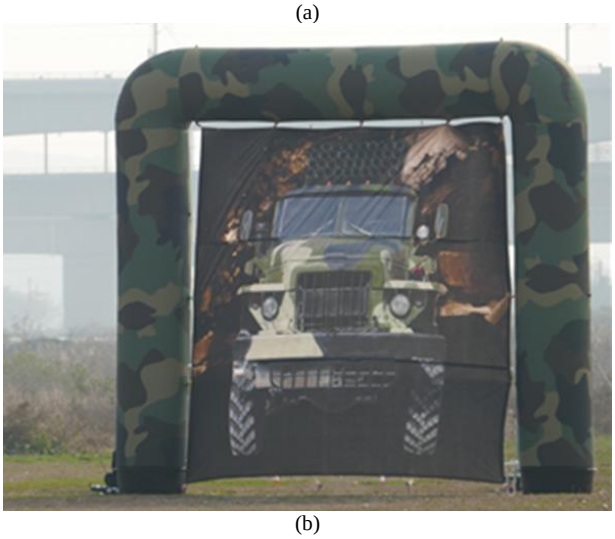

(b)

Fig. 1. (a) Target image, (b) Target realization result by using the inflatable material

Our proposed algorithm is possible to detect and track the target robustly in the real environment because it utilize the information consisting of not only the prior knowledge but also the inter-intra feature matching result. More detail part is described following section.

2.1 Target Sensing by using Point-like Feature Matching

To extract point-like features, the accelerated KAZE detector is applied. This scheme uses the explicit diffusion based on the multiple scharr filter embedded in a pyramidal framework and a modified local difference binary descriptor to detect features fast [1].

This scheme can detect more meaningful point-like features highly similar to corners whereas other schemes detect the useless features that not existing on the corner as shown in Fig. 2. Therefore, it does not require to the resampling features or the removing outlier algorithm too much in the feature matching step.

The adopted scheme is realized by using OpenCV 3.0a [2]. It supports the algorithm with the graphic processing unit (GPU) and we added the feature matching algorithm with the simple outlier removing scheme. The feature matching result is shown in Fig. 3.

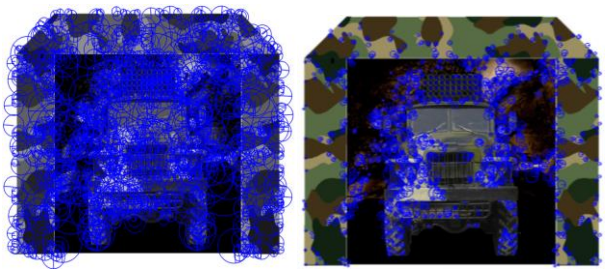

(a) (b)

Fig. 2. Point-like feature detection results (a: SURF, b: A-KAZE)

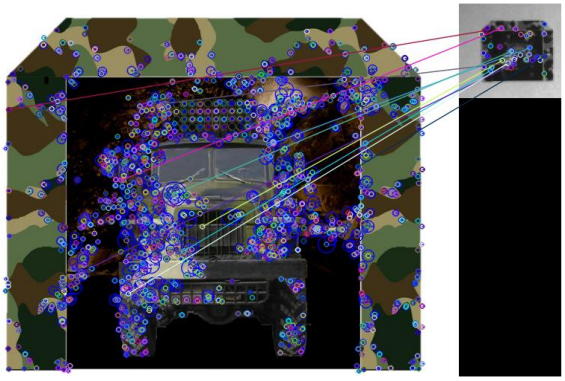

Fig. 3. Feature matching result using a prior-target image

2.2 Target Sensing by using Mean-shift Segmentation-based Edge Detection

The target sensing based on the feature matching may fail because the number of matched features are quite low in the large relative distance environment. In this case, the texture and edge information are useful to detect the target. However, there are many textures in the real environment such as a variety of colors or edge directions. Therefore, it is necessary to represent the texture briefly from the obtained image. In order to satisfy this need, the mean-shift segmentation augmented by GPU is applied [2]. It can shrink the number of represented textures by using some tuning parameters.

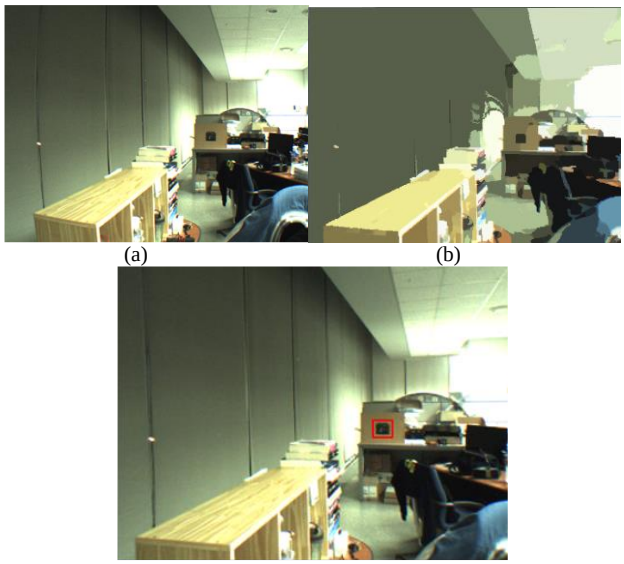

Fig. 4.(a) Source image, (b) Mean-shift segmentation result, (c) Designated target detection result

Furthermore, the edge information becomes more clearly in the location of complementary colors contrast and the otherwise thing is removed at the same time. By using this characteristic, we can apply the convex-hull-based contour detection algorithm with the simple outlier rejection scheme [2]. In this paper, we calculate the characteristics of the rectangular contour such as the rectangularity and some condition comparison scheme by using the area or perimeter calculation provided OpenCV are applied [3].

The segmentation and sensing result figures are shown in Fig. 4. (b)-(c). As shown in these figures, the expression of the environment`s texture level can effectively condensed. Furthermore, the segmentation algorithm can reduce significantly the edge information in the complex texture environment. Therefore, the target can be acquired more easily. The minimum detectable point is located at the 5.5[m] as the target size is A4 and at the 50-100 [m] with respect to the 4.0x4.0 [m] of the target size.

2.3 Target Tracking by using Kalman Filter

To track the target in the image plan, we adopted the Kalman filtering scheme. The system model is set up by using the constant speed assumption [4]. The measurement can get about 8[Hz] in the form of the rectangular shape of the region of interest (ROI). Something different from other scheme, we proposed the

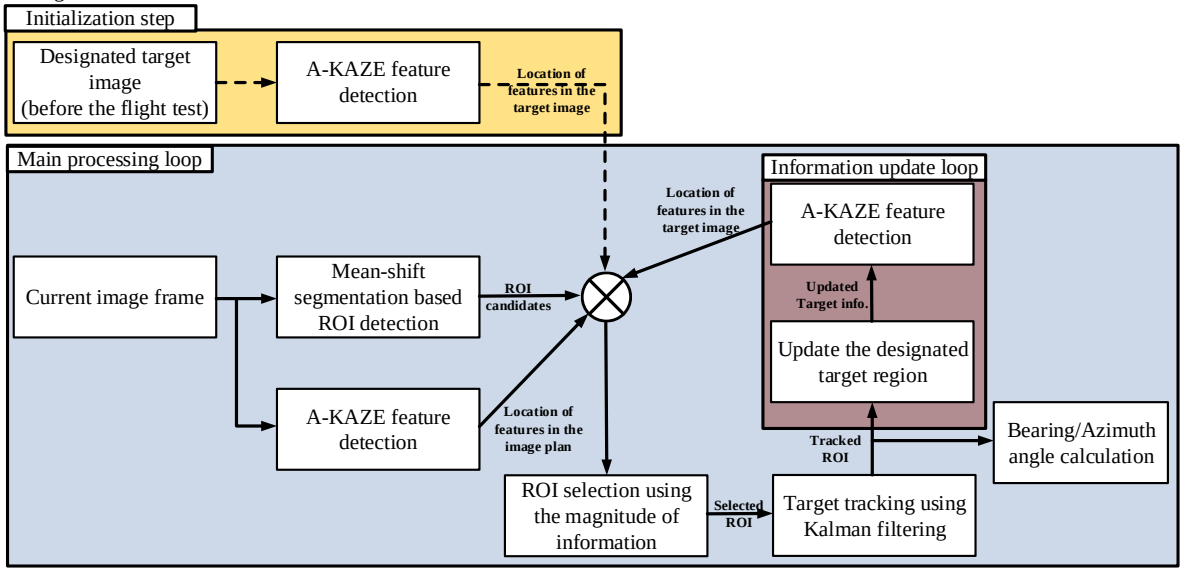

Fig. 5. Total flow chart of the proposed image processing algorithm

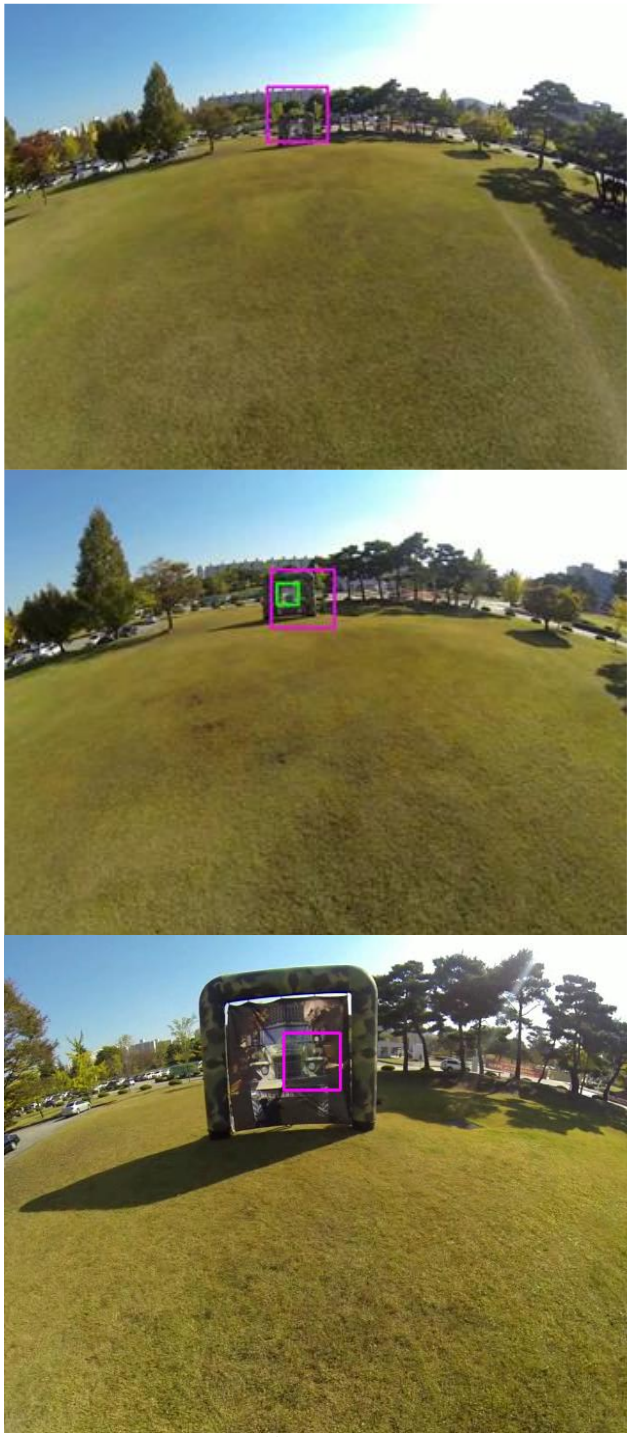

Fig. 6. The sequential images of the proposed image processing result

coarse-to-fine approach based on the magnitude of the information.

In detail, the target sensing by using mean-shift segmentation-based edge detection works fine in the large relative distance. However, the magnitude of the information is quite low because there are less matched features in the ROI. Therefore, it has low probability. Whereas in the short relative distance, the target sensing

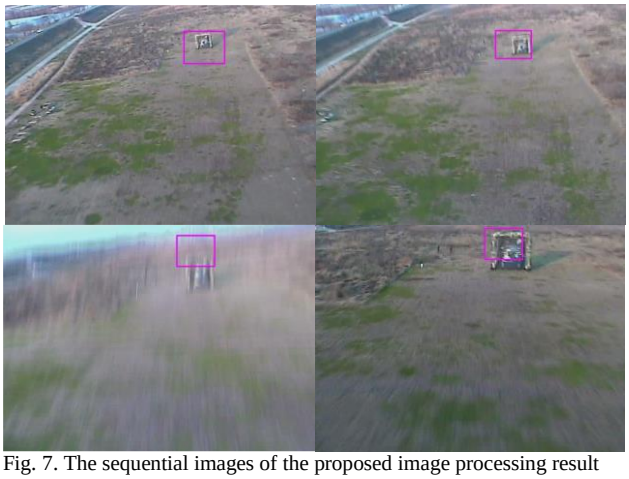

Fig. 7. The sequential images of the proposed image processing result from the approaching state

by using A-KAZE-based point-like feature matching works fine either and many features are matched compared with the large scale environment. Therefore, the small ROI can be derived and it has high probability. This characteristic is similar to the covariance.

The total flow chart of the proposed visual sensing algorithm is shown in Fig. 5.

Furthermore, the sequential images of the proposed image processing result are shown in Fig. 6-7. We obtain the expected result in the algorithm development phase. Although the severe blurr effect is occurred in the approaching step cause of the rapid pitching motion, the proposed algorithm works fine as shown in Fig. 7.

3 Time-to-Go-based Longitudinal Guidance Law with the Direct Visual Servoing

Generally, the glide slop angle for the fixed-wing UAV is 2-3°. However, our proposed scenario is aim to hit the designated target located at the front side or backward side by using the fixed-wing UAV as soon as possible.

Therefore, the estimated time-to-go based longitudinal control reference generation is applied [5-6]. The geometrical relationship for the calculation is shown in Fig. 8.

Furthermore, the direct visual servoing by using the target`s bearing and azimuth angle is developed for increasing performance in the terminal phase [7].

The time-to-go can be estimated by using the flight states as shown in Eq. (1).

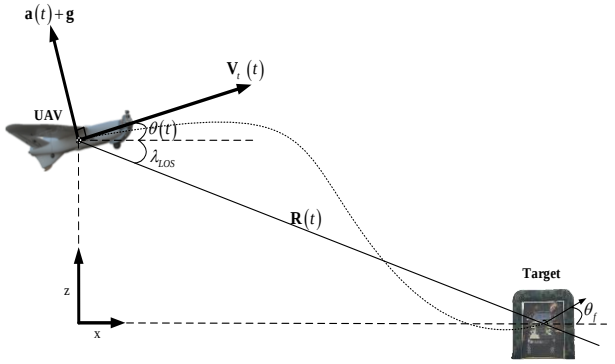

Fig. 8. The geometrical relationship for generating the longitudinal guidance law

$$t_{go} = t_f - t = \frac{R_{xz}}{V_t} = \frac{\sqrt{R_x^2 + R_z^2}}{V_t}$$
$$\hat{t}_{go} = \frac{R_{xz}}{V_t \cos(\gamma - \lambda_{LOS})} \quad (1)$$

where $\mathbf{R}$ is the relative distance vector, $\mathbf{V}_t(t)$ is the trim speed of the UAV, γ is the flight path angle, λ_{LOS} is the line-of-sight (LOS) angle and $\hat{t}_{go}$ is the estimated time-to-go value. Using Eq. (1), the vertical acceleration with respect to the body axis is approximated as follows.

$$a_z(t) = c_0 + c_1\hat{t}_{go} + c_2\hat{t}_{go}^2 \cdots \quad (2)$$

Without loss of generality, c_0 and c_1 are zero for satisfying the final condition, θ_f . Therefore, the vertical acceleration is modified as shown Eq. (3), the integrated result of Eq. (3) is shown as Eq. (4) and the coefficients are shown as Eq. (5) finally.

$$a_z(t) = c_m\hat{t}_{go}^m + c_n\hat{t}_{go}^n \quad (3)$$

$$V_z(t_f) = 0 = V_z(t_0) + g\hat{t}_{go} + \frac{c_m}{m+1}\hat{t}_{go}^{m+1} + \frac{c_n}{n+1}\hat{t}_{go}^{n+1}$$
$$R(t_f) = 0 = R(t_0) + V_z(t_0)\hat{t}_{go} + \frac{1}{2}g\hat{t}_{go}^2 + \frac{c_m}{m+2}\hat{t}_{go}^{m+2} + \frac{c_n}{n+2}\hat{t}_{go}^{n+2} \quad (4)$$

$$\therefore \begin{cases} c_m = \dfrac{(m+1)(m+2)}{n-m}\left[\dfrac{n+2}{\hat{t}_{go}^2}R(t_0) + \dfrac{V_z(t_0)}{\hat{t}_{go}} - \dfrac{1}{2}ng\right]\dfrac{1}{\hat{t}_{go}^m} \\ c_n = \dfrac{(n+1)(n+2)}{n-m}\left[-\dfrac{m+2}{\hat{t}_{go}^2}R(t_0) - \dfrac{V_z(t_0)}{\hat{t}_{go}} + \dfrac{1}{2}mg\right]\dfrac{1}{\hat{t}_{go}^n} \end{cases} \quad (5)$$

Therefore, the longitudinal acceleration term is derived as Eq. (6) and the reference angle of the pitch axis from time-to-go estimation is derived as Eq. (7),

$$\therefore a_{long}(t) = K_{long}\left\{\frac{(m+2)(n+2)}{(\hat{t}_{go})^2}R_z(t) + \frac{(m+n+3)}{(\hat{t}_{go})}V_z(t) - \frac{(mn-2)}{2}g\cos\theta\cos\phi\right\} \quad (6)$$
$$\left(\lambda_{LOS}(t) = \tan^{-1}\left\{\frac{R_z(t)}{R_x(t)}\right\}, \gamma = \theta - \alpha, \hat{t}_{go} = \frac{R_z}{V_t\cos(\gamma - \lambda_{LOS})}\right)$$

$$\therefore \theta_{ref}^{t_{go}}(t) = \tan^{-1}\left\{\frac{a_{long}(t)}{g_z}\right\} \quad (7)$$

Meanwhile, the direct visual servoing term is applied by using the target`s vertical position in the image plan for performing precision movement at the terminal phase [7]. The derived term is shown in Eq. and the total longitudinal guidance reference is calculated by using Eq. (8-9)

$$\theta_{ref}^{img}(t) = -K_{pitch}(v - \bar{v}) \quad (8)$$

$$\therefore \theta_{ref}(t) = \theta_{ref}^{t_{go}}(t) + \theta_{ref}^{img}(t) \quad (9)$$

Without loss of generality, the lateral guidance reference is modified by Eq. (10).

$$\therefore \psi_{ref}(t) = \psi_{ref}(t) + \psi_{ref}^{img}(t)$$
$$= \psi_{ref}(t) + K_{yaw}(u - \bar{u}) \quad (10)$$

where $\bar{u}, \bar{v}$ are the principal axis of the image plan. These guidance law is suitable for the fixed-wing UAV because it has the fast trim speed and the GPS-assisted midcourse guidance law. In detail, the fixed-wing UAV can hit the target applying the change of the relative movement from the visual sensing between the target and host vehicle when there is significant changes in the image plan during the terminal phase. The proposed algorithm can be performed by tuning some P-gain. It is simple, but has advantages that can be operated intuitively through the simple tuning.

4 Flight Test Results and Analysis

4.1 Flight Test Results

We performed the closed-loop flight tests by using the fixed-wing UAV. The scenario is the non-LOS type that the mission is engaged while the target is located backside of the UAV as shown in Fig. 10. (a). These results are acquired while cruising speed is 18[m/s] with the single GPS-aided navigation system and the wind speed is 5-8[m/s] respectively. We acquire ten times the total flight test results in one day as shown in Fig. 9.

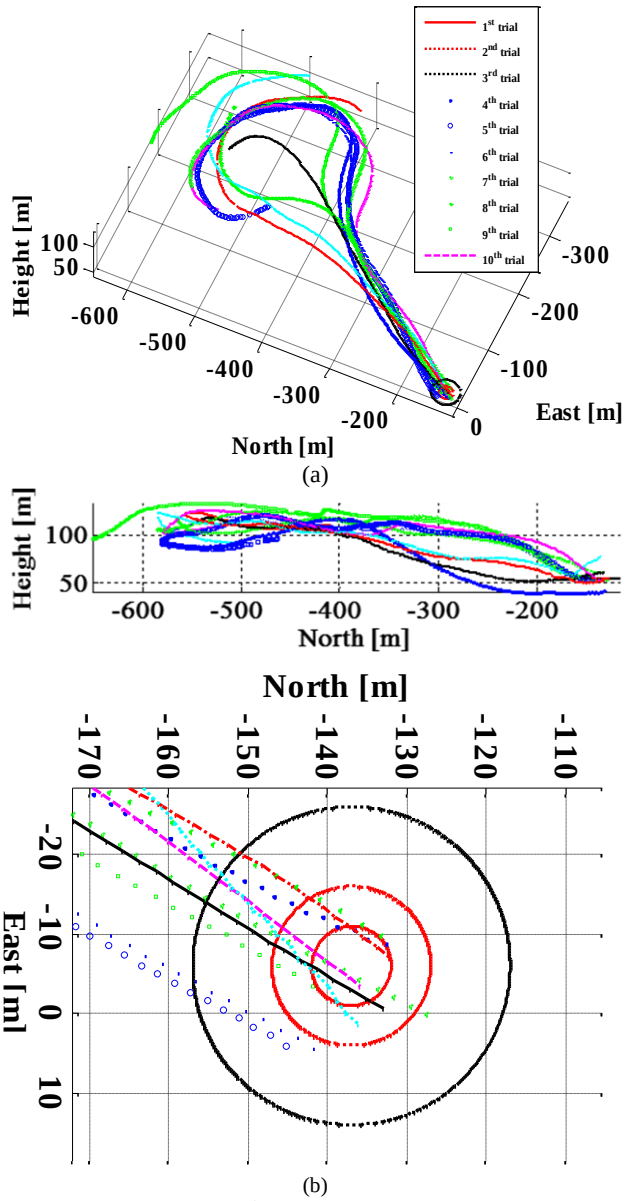

Fig. 9. (a) Flight trajectories for collecting the approaching and hitting the target, (b) Two-dimensional axis target approaching and hitting results

Our proposed guidance law`s input is the vertical acceleration with the estimated t-go parameter, not the height or gamma angle. Based on the results, the proposed guidance law can make the reference angle properly and the inner loop can follow it while the pitch angle reference is rapidly changing as shown in Fig. 10. (b)-(e).

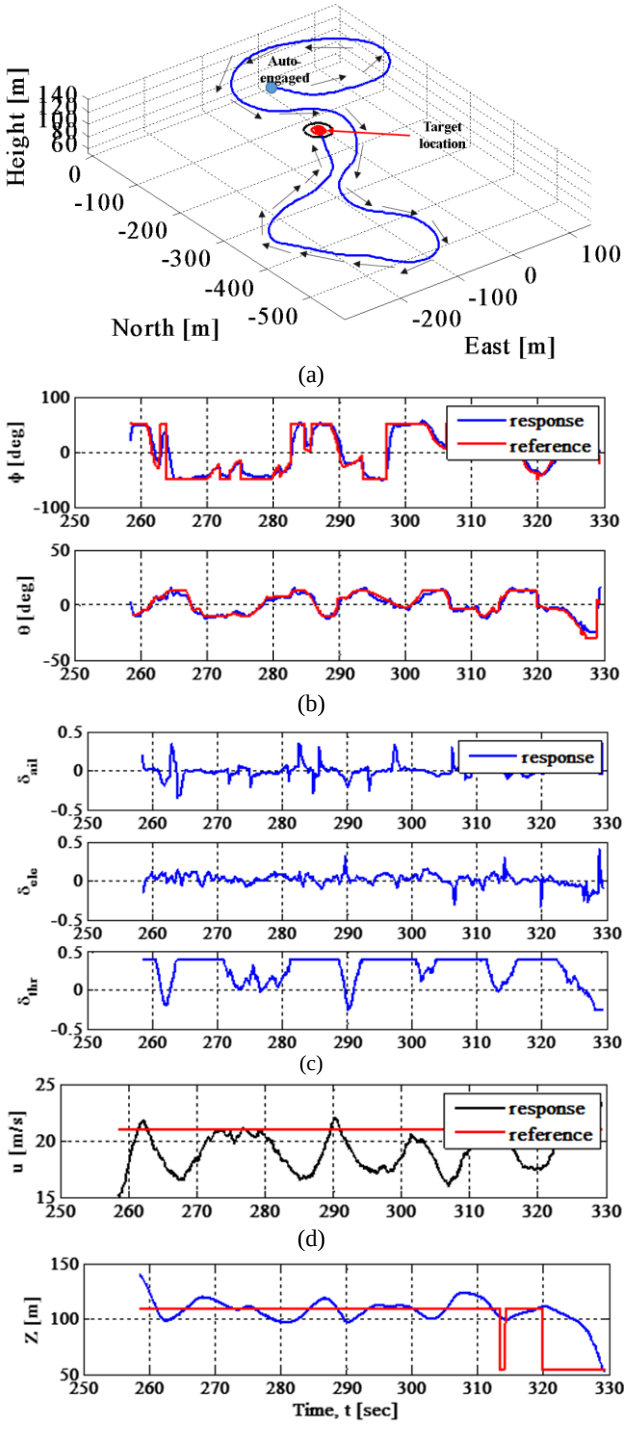

Fig. 10. Three dimensional trajectory(a) and the time histories of the flight states, (b) attitude control (inner loop) (c) control input, (d) air-speed control, (e) height control

4.2 Circular Error Probability Analysis

We analyze the flight test results based on the circular error probability (CEP) [8]. The data we used has two types: One is the flight data only and the other is that adding the virtual data by using the Gaussian distribution assuming that the tests are performed in the similar experimental environment. To do these data type, the elliptical shape approximated equation is used

$$R_{CEP} = 0.615\sigma_x + 0.562\sigma_y, \; if \;\; \sigma_x > \sigma_y \quad (11)$$

Based on the Eq. (11), we acquired the CEP results: xy-axis is 5.8905[m], xz-axis is 8.3402, yz-axis is 8.0212[m]. To consider removing the GPS error (UBlox LEA-6H, aiding performance, hor: 1~3[m], ver: 3~5[m]), the CEP with respect to each axis is 2.8905 [m] and 3.0212 [m]. This result can be analyzed to very effective with respect to the target size and the position accuracy. If the vehicle`s operational concept is the slug-type, not the precision hit, our proposed algorithm can be more appropriately.

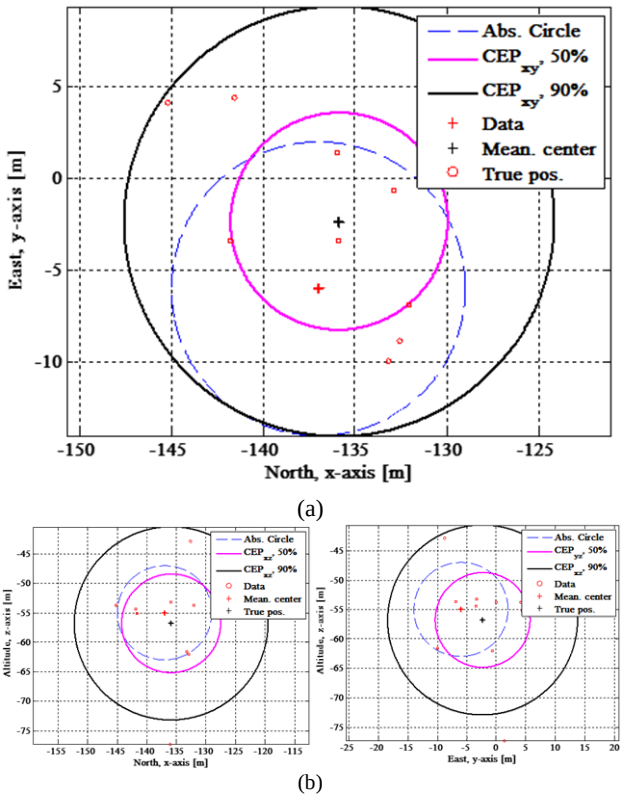

(a)

(b)

Fig. 11. (a) CEP calculation result in XY-axis (CEP 5.8905 [m]), (b) CEP calculation result in XZ (left) and YZ (right)-axis (8.3402 [m], 8.0212 [m])

5 Conclusion

Our proposed algorithm using the fixed-wing UAV is able to perform the mission much more inexpensively in the sense of the position accuracy instead of using the expensive smart bomb equipped on the fighter aircraft. Furthermore, our development system can be deployed quickly by the ground operator near the enemy`s site. Therefore, our proposed algorithm with UAV system is valuable in the manner of operability.

Acknowledgment

This work was supported by a national research foundation of South Korea (NRF) grant (No. 2012033464) funded by the South Korea government (Ministry of Science, ICT and Future Planning).

References

[1] Meixi Chen,Yule Yuan, Yong Zhao, "KAZE FeaturePoint with Modified-SIFT Descriptor", 3rd International Conference on Multimedia Technology, Nov., 2013
[2] OpenCV 3.0a, http://docs.opencv.org/3.0.0/
[3] Line and cross point equation, http://blog.daum. net/pg365
[4] Sungwook Cho, Sungsik Huh, Yeundeku Jung, D.H.Shim, "A Vision-based Road Following Scheme for Unmanned Aerial Vehicles", KSAS fall conference 2012, pp. 673-678, Nov., 2012
[5] Byoung-Mun Min, Min-Jea Tahk, David Hyunchul Shim and HyoChoong Bang, "Guidance Law for Vision-based Automatic Landing of UAV", KSAS International Journal, Vol. 8, No. 1, May, 2007
[6] T.Kim, C.Lee, Min-Jea Tahk, "Time-to-go Poly -nomial Guidance Law for Target Observability Enhancement", KSAS journal, Vol. 39, No. 1, pp.16-24, Jan., 2011
[7] Sungwook Cho, Sungsik Huh and David Hyunchul Shim, "Visual Detection and Servoing for Automated Docking of Unmanned Spacecraft", Trans. JSASS Aerospace Tech. Japan, Vol. 12, No. APISAT-2013, pp. a107-a116, Dec., 2014
[8] Vittal P. Pyati, "Computation of the Circular Error Probability (CEP) Integral", IEEE Trans. on Aerospace and Electronic Systems (TAES), Vol. 29, No.3, July, 1993

Copyright Statement